# INFLUENCE OF NIOBIUM ON STEADY-STATE CREEP BEHAVIOUR OF Ni-Cr-Ti TYPE WROUGHT SUPERALLOY

Encai Guo
Central Iron and Steel Research Institute,
Beijing, China

Zhiyan Han, Shuyou Yu
Research Institute of Steel Works,
Qiqihaer, China

## Summary

The steady-state creep rate, $\dot{\varepsilon}_s$, the stress-exponent, n, and the apparent creep activation energy, Qapp, of the alloys with various Nb contents were determined. Effect of various microstructure parameters of these alloys on $\dot{\varepsilon}_s$ was studied. The following equations were obtained:

$$Q_{app} = Be^{Kx/\log e}$$

$$\dot{\varepsilon}_s = A_1 L^b \gamma_{SFE}^{\alpha} \sigma^n \exp(-\frac{Q_{app}}{RT})$$

The TEM observation of thin foil shows that the basic creep mechanism is plane slip due to the motion of the dislocation cutting $\gamma'$ phase under the condition investigated.

## Introduction

In an earlier paper[1] the authors reported that the presence of niobium strengthens Ni-Cr-Ti type superalloys by solid-solution hardening and $Ni_3(Al,Ti,Nb)$ precipitation hardening due to increasing the volume fraction, the particle radius and the long-range order parameter of $\gamma'$, so that the yield stress of the alloys containing Nb is obviously increased. Effect of Nb on steady-state creep behaviour is also very interesting. The present investigation was carried out to study steady-state creep behaviour of the alloys with various Nb contents in the temperature range of 700-760° C and the stress range of 392-509.6 $MNm^{-2}$.

## Experimental Procedure

The parent alloy was vacuum induction melted with the composition (in wt.%) of C 0.04, Al 0.95, Ti 2.9, Cr 20.0, B 0.01, Ce 0.01, Ni bal. Different amounts of Nb and a small quantity of c, Ti and Mn were added to the parent alloy when it was remelted by vacuum induction, then a group of experimental alloys was obtained. The percentage contents of Nb in the alloys are shown in table I. The ingots were hot rolled to bars. Before machining specimen, the bars were heat treated by 1080°C, 8hr. A.C., 750°C, 16hr. A.C.

A lever-type constant-load creep test machine was utilized for the test. The total length, the diameter of parallel part and the gauge length of the specimen are 167, 8 and 100mm, respectively. During the test, the temperature was controlled to within ± 2°C, the accuracy of deformation measurement was 0.5$\mu$m. The stress was not constant during the test because the constant-load machine was used. Thus it is necessary to correct the steady-state creep rate, $\dot{\varepsilon}_s$, measured. The correction formula, as follows, is used[2]:

$$\eta^* = \eta - \frac{1}{2}(n+1)\eta^2 + \frac{1}{6}(n+1)(n+2)\eta^3 \qquad (1)$$

Where $\eta$ is strain rate measured during test, $\eta^*$ is strain rate corrected, n is stress exponent determined by following equation:

$$n = [d\,Ln\dot{\varepsilon}_s / d\,Ln\,\sigma\,]_{T=const.} \qquad (2)$$

Both the experimental methods of varying $\sigma$(T=const.) and varying T($\sigma$=const.) with single specimen were utilized to measure $\dot{\varepsilon}_s$ value varying with the stress and test temperature[2]. The least-square was used to determine n value and apparent activation energy, Qapp. After proceeding well into the steady-state regimes, the tests were stopped and specimens were cooled under the load to minimize the recovery of the deformation.

Thin foils were made from specimens after creep test and examined by using EM-400 transmission electron microscope.

## Experimental Results

Creep curves of the alloys with different Nb contents at 700°C under 441 $MNm^{-2}$ are shown in Fig.1. $\dot{\varepsilon}_s$ and the plastic strain, p, of the alloy without Nb(No.1) are $10\times10^{-5}$/h and 0.96%, respectively. It is found that the tertiary creep stage appeared after 50hr. for the alloy without Nb. However $\dot{\varepsilon}_s$ and p of the alloys with different Nb contents are within (1.6 to 2.8)$\times10^{-5}$/h and (0.19 to 0.25)%, respectively. And they still

belong in the secondary creep stage in 100hr. Thus it is obvious that the presence of Nb makes the creep rate and the plastic strain of the alloys decrease.

The relation between $\dot{\varepsilon}_s$ of the alloys and stress at 700°C under 392-509.6 $MNm^{-2}$ is shown in Fig.2. It is seen from Fig.2 that $Ln\dot{\varepsilon}_s$ is linear with $Ln\sigma$, then

$$\dot{\varepsilon}_s \propto \sigma^n \qquad (3)$$

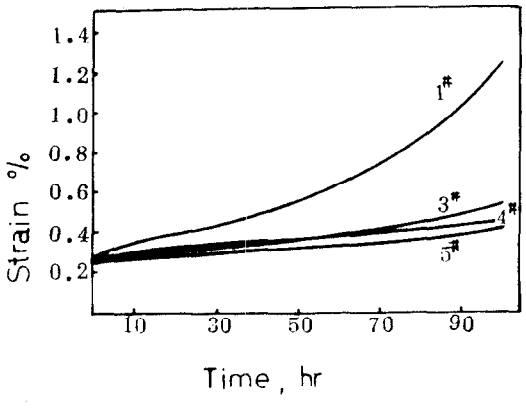


Fig.1 Creep curve of the alloys with various Nb contents.

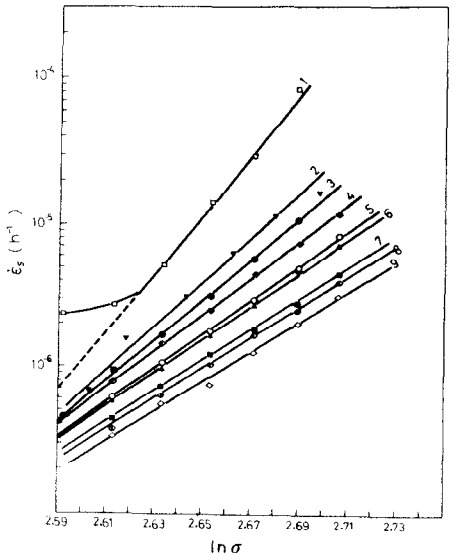


Fig.2, Steady-state creep rate VS stress (1-9 denoting specimens with various Nb contents)

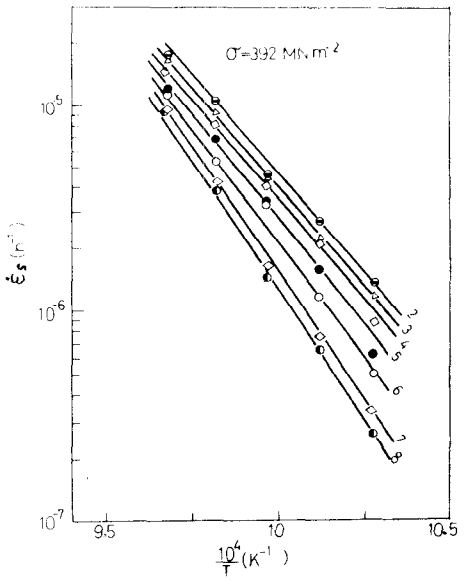


Fig.3 Steady-state creep rate of the alloys with Nb VS temperature

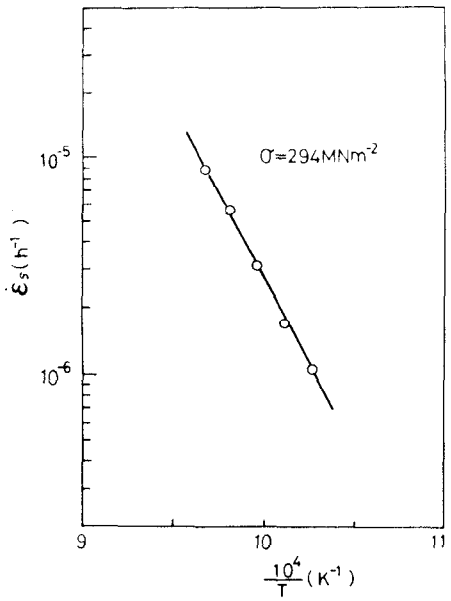


Fig.4 Steady-state creep rate of the alloy without Nb VS temperature

Variety of $\dot{\varepsilon}_s$ for the alloys containing various Nb contents with temperature within 700-760°C under 392MNm$^{-2}$ are shown in Fig.3, that for the alloy without Nb under 294MNm$^{-2}$ is shown in Fig.4

In order to find the dependence of creep behaviour on microstructure of these alloys, structure factors of the alloys with normal heat treatment are shown in tableI, which contains the average grain size, the stacking fault energy, $\gamma_{sFE}$ , of $\gamma$ materix and the volume fraction, f, particle radius and long-range order parameter, s, of $\gamma'$

Table 1 Structure factors of the alloys with various Nb contents

| No. | Nb content wt.% | average grain size, L,$\mu$m | $\gamma$-stacking fault energy, $\gamma_{sFE}$Jcm$^{-2}$ | $\gamma'$-particle radius, Å | $\gamma'$-long-range orders, s | $\gamma'$-volume fraction f % |
|---|---|---|---|---|---|---|
| 1 | - | 87.76 | $63.2\times10^{-7}$ | 84.5 | 0.79 | 12.56 |
| 2 | 0.51 | 60.70 | $62.8\times10^{-7}$ | 85.5 | 0.82 | 12.98 |
| 3 | 1.00 | 54.96 | $61.4\times10^{-7}$ | 98.5 | 0.85 | 14.18 |
| 4 | 1.24 | 54.95 | $60.5\times10^{-7}$ | 101.5 | 0.86 | 14.85 |
| 5 | 1.53 | 49.80 | $59.1\times10^{-7}$ | 98.5 | 0.87 | 14.84 |
| 6 | 1.72 | 44.74 | $58.5\times10^{-7}$ | 98.5 | 0.92 | 14.95 |
| 7 | 1.94 | 38.52 | - | 92.5 | 0.95 | 15.91 |
| 8 | 2.46 | 34.95 | $54.6\times10^{-7}$ | 113 | 1.01 | 16.21 |
| 9 | 2.75 | - | - | - | - | - |

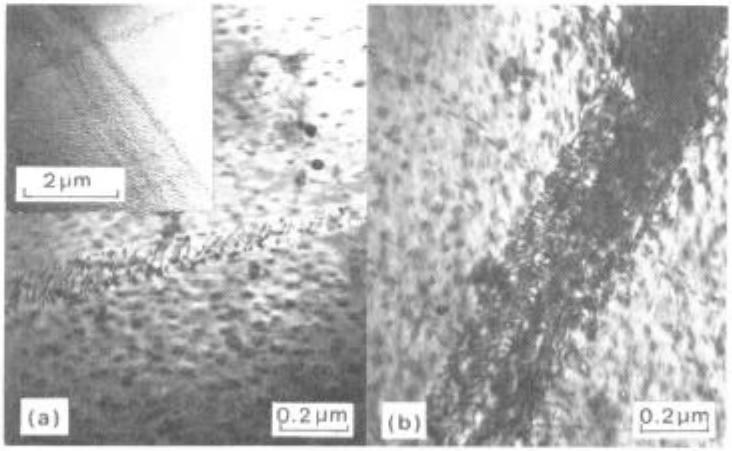


Fig.5 Plane slip bands (A) and dislocation cutting $\gamma'$ phase in slip bands (A and B)

The thin foil observations for specimens after creeping within temperature and stress range investigated show that there were a lot of plane slip bands observed under low magnification and dislocations cutting through $\gamma'$ within slip bands while under high magnification Fig.5 (a,b) . This suggests that under the conditions investigated, the mechanism controling creep of the alloys is basically the plane slip due to the motion of the dislocation cutting $\gamma'$.

## Discussion

1. Temperature dependence of steady-state creep rate

A group of straight lines of $\mathrm{Ln}\,\dot{\varepsilon}_s$ against $\frac{10^4}{T}$ for the alloys with various Nb contents and for the alloy without Nb were respectively shown in Fig.3 and 4. These straight lines are very nearly parallel each other. It indicates that the rate-controlling thermal-activation process is independent of stress level and exponential relation exists between steady-state creep rate and temperature as follows

$$\dot{\varepsilon}_s = A\,\sigma^n \exp(-\frac{Qapp}{RT}) \qquad (4)$$

A group of calculated Qapp and n values for the alloys is shown tableII. Fig.6 shows a plot of LogQapp against Nb content in the alloys. It is found that Qapp is given by the following equation

$$Q_{app} = B e^{kx/\mathrm{Log}e} \qquad (5)$$

where x is atomic percentage of Nb in the alloys, k is the slope and about equal to 0.11, B is the intercept and about equal to 77.62.

TableII Qapp and n values of the alloys with various Nb contents

| No. | Qapp, KJmol$^{-1}$ | n |
|---|---|---|
| 1 | 308 | 16.09 |
| 2 | 352 | 14.73 |
| 3 | 378 | 13.78 |
| 4 | 389 | 13.07 |
| 5 | 414 | 12.13 |
| 6 | 435 | 11.83 |
| 7 | 443 | 10.78 |
| 8 | 471 | 10.22 |
| 9 | 497 | 9.71 |

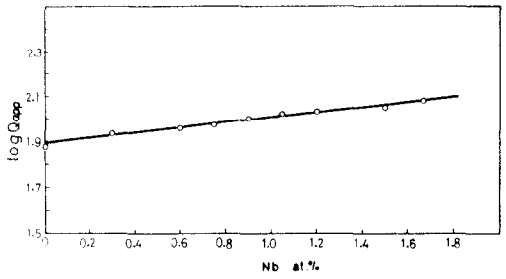


Fig.6 LogQapp VS Nb content in the alloys

2. Relation between steady-state creep rate and $\gamma$ matrix strengthened by niobium

The grain size, L, of the alloys and the stacking fault energy, $\gamma_{sFE}$, of $\gamma$ matrix decrease with increasing Nb content in the alloys as showing in Tab.I. Fig.7 gives a plot of $\dot{\varepsilon}_s$ against L. It is found that for a given temperature $\dot{\varepsilon}_s$ decreases with decreasing L. There is a relation, as follows, within the range of temperature from 0.6 to 0.64 Tm

$$\dot{\varepsilon}_s \propto L^b \qquad (6)$$

where Tm is the melting point of the alloy, b depends on test temperature. At 700 and 760°C, b is about 2.55 and 1.13 respectively. The intercept of the straight line increases with increasing temperature. $\mathrm{Log}\,\gamma_{sFE}$ is plotted against $\mathrm{Log}\,\dot{\varepsilon}_s$ in Fig.8. It was found from Fig.8 that there is a relation as follows

$$\dot{\varepsilon}_s \propto \gamma_{SFE}^{\alpha} \qquad (7)$$

where $\alpha$ decreases with increasing temperature, from 11.76 at 700°C to 5.58 at 760°C. However the effect of temperature on intercept of straight line

is more obvious.

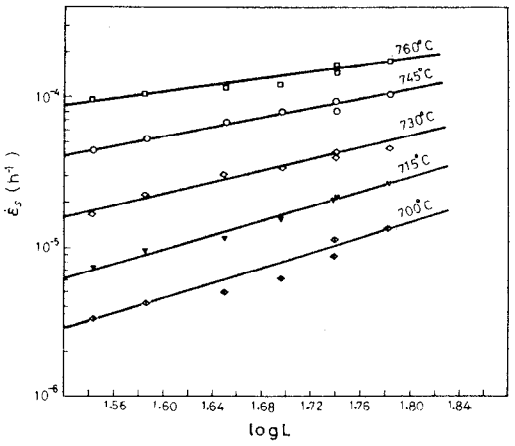


Fig.7, Steady-state creep rate VS grain size

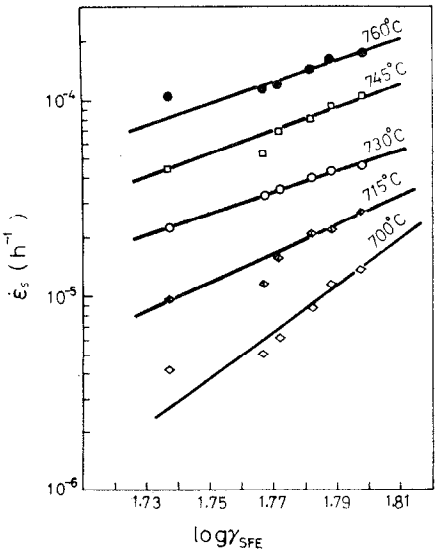


Fig.8 Steady-state creep rate VS stacking fault energy, $\gamma_{SFE}$, of $\gamma$ matrix

If the grain size and stacking fault energy are regarded as parameters of solid solution strengthening[3] there would be a relation as follows

$$\dot{\varepsilon}_s = A_1 L^b \gamma_{SFE}^{\alpha} \sigma^n \exp(-\frac{Q_{app}}{RT}) \qquad (8)$$

3. Relation between steady-state creep rate and $\gamma'$-phase strengthened by Nb

As above, the mechanism controlling creep of the alloys is plane slip caused by dislocation moving and cutting through $\gamma'$. Thus dispersion parameters ( $\gamma'$ particle size and spacing between $\gamma'$ particles) and $\gamma'$ particle strength must influence the steady-state creep rate directly. In the investigated alloys, Nb distributes in $\gamma$, $\gamma'$ and carbide with the approximate ratio of 5:3:1[1]. However owing to the $\gamma'$ -volume fraction in the alloys being only about 10%, the concentraction of Nb in $\gamma'$ is about 3 times as high as that in $\gamma$. The volume fraction, particle size and long-range order of $\gamma'$ are increased by adding Nb, hence the obstacle to dislocation motion during deformation is reinforced, the average free distance for dislocation slip is shortened and the resistance to dislocation cutting through $\gamma'$ is increased. It is interesting to induce an effective stress $(\sigma-\sigma_b)$ to describe steady-state creep rate. $\sigma_b$ is back stress[4] which is characteristic of the material microstucture. It will be discussed further in future paper .

4. Observation on slip deformation during ceep

The dislocation cutting through $\gamma'$ in slip band and the superlattice dislocation pair are shown in Fig.5. The diffraction pattern corresponding to Fig.5b is shown in Fig.9. It was obtained from Fig.9 that the trace direction corrected by magnetic rotation angle is $[2\bar{1}\bar{3}]$ and the slip plane is (111). The diffraction vectors, $\vec{g}_1=[3\bar{1}\bar{1}]$, $\vec{g}_2=[20\bar{2}]$ after dislocation contrast disappearing was obtained from Fig.10, then the Burgers vector, $\vec{b}$, was calculated to be equal to $[1\bar{2}1]$. The projection spacing,e,between the paired dislocations in the foil surface was measured to be about 140-229Å

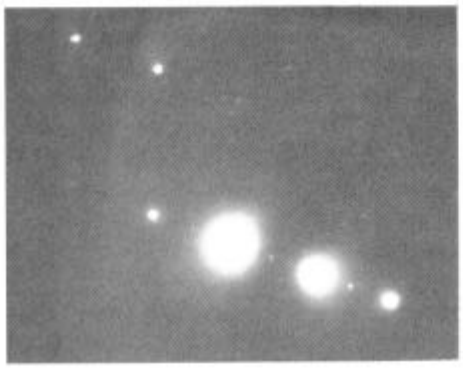

Fig.9(a) The diffraction pattern of Fig 5b

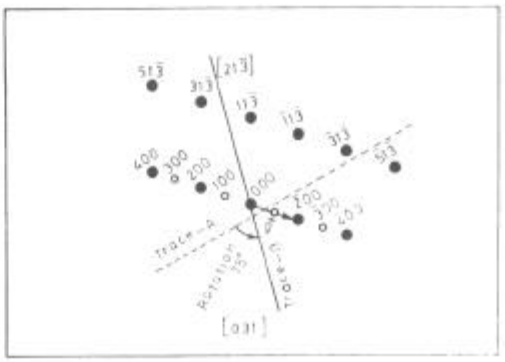


Fig.9(b) Indexing for 9(a)

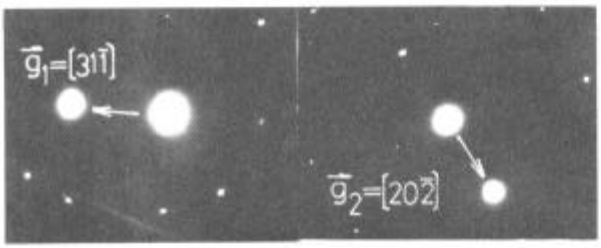


Fig.10. The diffraction pattern after the dislocation contrast the first and the second disappearing

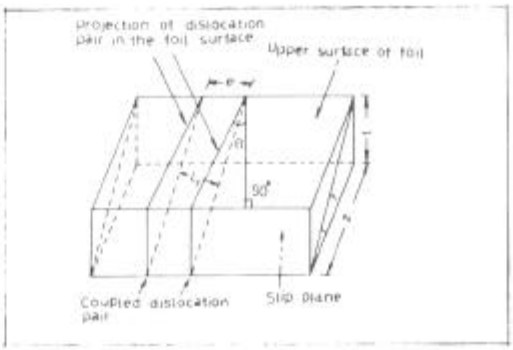


Fig.11. Geormetric relation to find true perpendicular distance $L_1$ between dislocation pairs in thin foil

(Fig.11). The true normal distance, $L_1$, between the dislocation pairs in slip plane was obtained by the following relation[5]

$$L_1 = e \cos\left[\tan^{-1}(\tan\beta \cos\gamma)\right] \qquad (9)$$

It is about 100-165 Å, which is very close to the $\gamma'$ particle size measured (Tab.I). It seems that $\frac{a}{2}[1\bar{1}0]$ complete dislocation is dissociated into $\frac{a}{6}[1\bar{2}1]$ and $\frac{a}{6}[2\bar{1}\bar{1}]$ partial dislocations when it cuts through $\gamma'$. The APB energy between paired dislocations increases with increasing $\gamma'$ long-range order, Nb in $\gamma'$ elevates the slip deformation resistance and decreases the steady-state creep rate, finally increases the creep resistance of the alloys.

## Conclusion

1. The presence of Nb in Ni-Cr-Ti type alloy makes the grain size of the alloy fine, the stacking fault energy of $\gamma$ matrix decrease and the volume fraction, particle radius and long-range order parameter of $\gamma'$ increase.

2. The stress exponent, n, decreases, Qapp increases with increasing

Nb content in the alloy. The value Qapp obeys the following relation

$$Q_{app} = B\, e^{kx/\mathrm{Log}\, e}$$

3. In the range of temperature and stress investigated $\dot{\varepsilon}_s$ obeys

$$\dot{\varepsilon}_s = A_1 L^b\, \gamma_{SFE}^{\alpha}\, \sigma^n \exp\left(-\frac{Q_{app}}{RT}\right)$$

4. The TEM observation of thin foil shows that $\frac{a}{2}[1\bar{1}0]$ complete dislocation in (111) slip plane is dissolved into $\frac{a}{6}[1\bar{2}1]$ and $\frac{a}{6}[2\bar{1}\bar{1}]$ partial dislocations when it cuts through $\gamma'$. The distance between superlattice dislocation pairs is about 100-165Å which very closes to $\gamma'$ particle size measured.

5. Under the test condition of the present work the basic creep mechanism is planar slip due to the motion of dislocations cutting the $\gamma'$ phase.

## References


1. Encai Guo and Fujin Ma, "The strengthening effect of niobium on Ni-Cr-Ti type wrought superalloy, " Superalloys 1980, Proc. of the Fourth Int. Symp. on Superalloys, Edited by J.K.Tien, et al, ASM, Metals Park, Ohio, 1980, pp431-438.

2. Chi Chen, et al, "The creep and stress-rupture properties of $\gamma'$crystals," Acta Physica Sinica, 23(1) (1974) p69.

3. O. Ajaja, T.E.Howson, S.Purushothaman and J.K.Tien, "The role of the alloy matrix in the creep behaviour of particle-strengthened alloys", Mater. Sci. and Eng. 44(2) (1980) P165.

4. S.Purushothaman and J.K.Tien, "Role of back stress in the creep behaviour of particle strengthened alloys, "Acta Met., 26(4) (1978) P519.

5. M.J.Marcinkowski,et al, "Dislocation configurations in $AuCu_3$ and AuCu type superlattices," Acta Met. 9(1961) P129.